Fracture Toughness of Closed-Cell Polymeric Foam under Mixed-Mode I/II Loading

Piyamon Poapongsakorn[1,*] and Chaosuan Kanchanomai[1]

[1] Department of Mechanical Engineering, Faculty of Engineering, Thammasat University, Pathumthani, Thailand 12120

* Corresponding Author: Tel: 02-564-3001, Fax: 02-564-3010,

E-mail: 5110300042@student.tu.ac.th

Abstract

Closed-cell polymeric foams are widely used as core materials in sandwich structures. During services, the structures might experience complex loading situations. Moreover, pores in the closed-cell foam could be the locations for initial defects or cracks in the structure. Thus, failure of polymeric foam is usually dominated by crack coalescence and propagation under mixed-mode loading. In this study, the mixed-mode (mode I/II) fracture behaviors of closed-cell PVC foam were investigated under various mode-mixity angles (β = 0° to 90°), i.e. the β is 0° for pure mode I loading, and becomes 90° for pure mode II loading. Single-edge notched bending specimens with 10-mm thickness were used in the present work. The tests were carried out at loading rate of 10^{-1} mm/min. It was found that K_{IQ} decreased with increasing mode-mixity angle. While, K_{IIQ} increased with increasing mode-mixity angle from 0° to 45°, and became insensitive to the change of the mode-mixity angle above 45°. Moreover, the fracture toughness of the PVC foam under dominated mode I loadings (β < 45°) was higher than that under dominated mode II loadings (β > 45°) due to the contraction in thickness direction and crack tip blunting at the dominated mode I loadings. These fracture mechanisms corresponds to the observation of fracture surfaces.

***Keywords**:* closed-cell polymeric foam, single-edge notched bending, fracture, mixed-mode I/II loading

1. Introduction

Due to light weight and high energy absorption, closed-cell polymeric foams are commonly used as core materials in sandwich structure for various engineering purposes, such as wing structure of aircraft and marine structures. However, the failure mostly occurs in the foam core since it has low strength. In addition, a number of pores in the foam could be the locations for initial defects which can coalesce and grow as a main crack and lead to the fracture of specimen. Thus, the fracture behavior of closed-cell polymeric foams has to be concerned. Viana and Carlsson [1] studied mode I fracture toughness (K_{Ic}) of polyvinyl chloride (PVC) foams with various thicknesses. They found that K_{Ic} decreases with decreasing specimen size i.e. fracture toughness of thinner specimens is lower than that of thicker specimens. Kabir et al. [2] have investigated fracture behavior under opening mode (mode I loading) of PVC and polyurethane (PU) foams. They found that K_{Ic} is dependent of loading rate and foam density.

However, during services, the structures are normally operated under complex loading. Thus, loading condition around the defect or crack is likely to be mixed-mode loading. Unfortunately, only a few works on fracture under mixed-mode loading of closed-cell polymeric foams have been done. Fracture behavior of PVC foams under mixed-mode I/II loading has been studied by Noury et al. [3] They found that the pure mode II fracture toughness (K_{IIc}) is significantly lower than the pure mode I fracture toughness (K_{Ic}). However, no work has given a clear explanation about the fracture mechanisms of closed-cell polymeric foams under various mixed-mode loading. Moreover, the structures are commonly used in the applications, such as pressure vessel, marine structure, and shipping container, for which the foam might experience the time-dependent effect due to the low loading rate.

The objectives of this work are to study the fracture behaviors of the closed-cell PVC foam under mixed-mode I/II loading as well as to clarify the fracture mechanisms of the foam under various mixed-mode loadings and low loading rate of 10^{-1} mm/min.

2. Experimental procedure

The PVC foam (DIAB H130) was used in this study. The density reported by the manufacturer was 130 kg/m^3. However, it was found that the foam density varies in a range of 100 to 130 kg/m^3 through the thickness of the foam panel. The variation in density could occur from the manufacturing process of the foam. The SEM micrograph of the PVC foam is shown in Fig. 1.

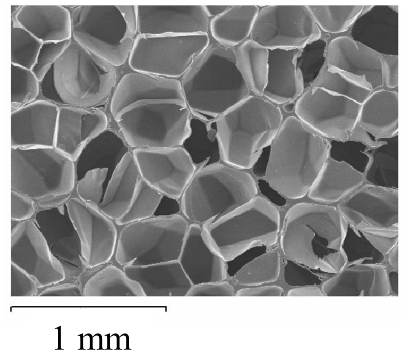

Fig. 1 SEM micrograph of PVC foam H130

For mixed-mode I/II fracture toughness, the mode-mixity angle (β) is used to define loading condition around the tip of crack. β can be defined as

$$\beta = \tan^{-1}\left(\frac{K_{II}}{K_I}\right) \tag{1}$$

where K_I is the stress intensity factor under opening mode (mode I) loading and K_{II} is the stress intensity factor under shearing mode (mode II) loading. The β is 0° for pure mode I loading and becomes 90° for pure mode II loading.

In this study, all fracture toughness tests were performed using single edge-notched bending (SENB) specimen [4] on a servo-hydraulic testing machine at 55% relative humidity and a constant temperature of 25°C. The specimens with the thickness (b) of 10 mm and the loading rate of 10^{-1} mm/min were applied. During the tests, the crack tip region of the specimens was observed using a travelling microscope connected with a digital camera. After failure, fracture surfaces were analyzed using scanning electron microscope (SEM).

In the experimental study, four types of fracture toughness tests were carried out in order to obtain various modes of loading around the crack tip (Fig. 2). All loading configurations of the mixed-mode I/II fracture toughness tests as well as the obtained mode-mixity angle (β) are summarized in Table. 1.

4-point bending test for mode I fracture toughness (4PBT-I)

For mode I loading, 4PBT was chosen to avoid localized deformation near the crack tip and crack propagation path (Fig. 2(a)). Symmetric loading was applied to a symmetric pre-cracked specimen. K_{IQ} for pure mode I loading can be determined as follows [5]:

$$K_{IQ} = \sigma_c \sqrt{\pi a} \cdot F(\alpha) \tag{2}$$

$$\sigma_c = \frac{3P_c L}{tW^2} \tag{3}$$

$$F(\alpha) = 1.122 - 1.121\alpha + 3.740\alpha^2 + 3.873\alpha^3 - 19.05\alpha^4 + 22.55\alpha^5 \tag{4}$$

where σ_c is the maximum applied stress calculated using beam theory, $F(\alpha)$ is the geometric function in the term of α ($\alpha = a_o / W$), and P_c is the maximum applied load.

3-point bending test of asymmetric pre-cracked specimen (3PBTA)

In this testing configuration, the mode mixity around the crack tip can be varied by adjusting the distance (s), as well as initial crack size (a_o) as shown in Fig. 2(b). K_{IQ} and K_{IIQ} can be determined as follows [6]:

$$K_{IQ} = \sigma_c F_I \sqrt{\pi a_o} \tag{5}$$

$$K_{IIQ} = \sigma_c F_{II} \sqrt{\pi a_o} \tag{6}$$

$$\sigma_c = \frac{3P_c A}{W^2 b} \tag{7}$$

$$F_I = F_I' \cdot (1-\alpha)^{-\frac{3}{2}} \tag{8}$$

$$F_{II} = F_{II}' \cdot (1-\alpha)^{-\frac{1}{2}} \tag{9}$$

where σ_c is the maximum applied stress calculated using beam theory, F_I' and F_{II}' are the geometric functions in the term of α ($\alpha = a_o / W$) [6], and P_c is the maximum applied load. Noted that for the distance $s = 0$, pure mode I loading can be obtained.

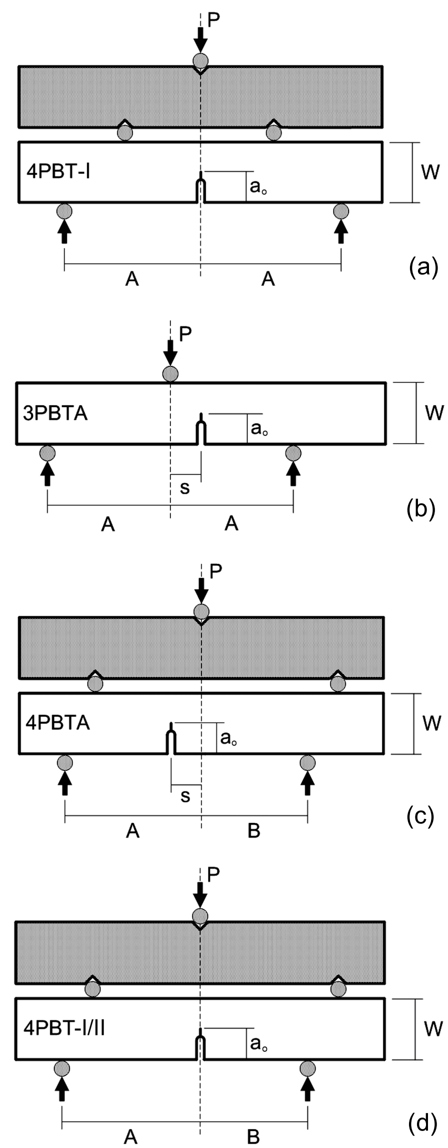

Fig. 2 Fracture toughness test configurations

Table. 1 Loading configurations of mixed-mode I/II fracture toughness tests

Fracture toughness test	a_o/W	*S* (mm)	*A* (mm)	*B* (mm)	β^o
4PBT-I	0.5	0	40	-	0
3PBTA	0.4	24	40	-	10
4PBTA	0.5	5	40	20	23
	0.5	3	40	20	30
	0.6	1.5	40	20	45
	0.7	1	40	20	60
	0.5	1	40	20	64
4PBT-I/II	0.3	0	50	10	80
	0.8	0	50	10	90

4-point bending test of asymmetric pre-cracked specimen (4PBTA)

The mixed-mode stress intensity factor around vicinity of crack tip can be manipulated by adjusting the distance (s), as well as initial crack size (a_o) as shown in Fig. 2(c). K_{IQ} and K_{IIQ} can be determined as follows [7]:

$$K_{IQ} = \sigma_c \sqrt{\pi a_o} \cdot F_I(\alpha) \quad (10)$$

$$K_{IIQ} = \tau_c \sqrt{\pi a_o} \cdot F_{II}(\alpha) \quad (11)$$

where σ_c is the maximum applied normal stress, and τ_c is the maximum applied shear stress which can be defined as follows:

$$\sigma_c = \frac{A-B}{A+B} \cdot \frac{6sP_c}{bW^2} \quad (12)$$

$$\tau_c = \frac{A-B}{A+B} \cdot \frac{P_c}{bW} \quad (13)$$

F_I and F_{II} are the geometrical functions given by He and Hutchinson [8] as follows:

$$F_I(\alpha) = 1.122 - 1.121\alpha + 3.740\alpha^2 + 3.873\alpha^3 - 19.05\alpha^4 + 22.55\alpha^5 \quad (14)$$

$$F_{II}(\alpha) = \frac{\alpha}{\sqrt{\pi(1-\alpha)}} \begin{bmatrix} 7.264 - 9.37\alpha + 2.74\alpha^2 \\ +1.87\alpha^3 - 1.04\alpha^4 \end{bmatrix} \quad (15)$$

while $\alpha = a_o/W$.

4-point bending test of symmetric pre-cracked specimen (4PBT-I/II)

The mixed-mode stress intensity factor around the crack tip vicinity can be manipulated by varying the initial crack size (a_o) as shown in Fig. 2(d). K_{IQ} and K_{IIQ} can be determined as follows [5]:

$$K_{IQ} = F_I \tau_c \sqrt{\pi a_o} \quad (16)$$

$$K_{IIQ} = F_{II} \tau_c \sqrt{\pi a_o} \quad (17)$$

$$\tau_c = \frac{P_c}{Wb}\left(\frac{1-B/A}{1+B/A}\right) \quad (18)$$

$$F_I(\alpha) = 0.6504 - 2.5807\alpha + 3.9417\alpha^2 - 2.1689\alpha^3 \quad (19)$$

$$F_I(\alpha) = -0.2915 + 6.3229\alpha - 9.1199\alpha^2 + 6.0570\alpha^3 \quad (20)$$

where τ_c is the maximum applied shear stress, F_I and F_{II} are the geometrical functions in the term of α ($\alpha = a_o/W$), and P_c is the maximum applied load.

3. Results and discussion

3.1 Load-deflection relationship

The relationships between load and deflection of the specimen tested under pure mode I loading and pure mode II loading are shown in Fig. 3. Under pure mode I loading, the evidence of plastic deformation (non-linear stage) was observed before the fracture occurred. However, the relationship of load and deflection under pure mode II loading was linearly increased until the unstable crack propagation occurred.

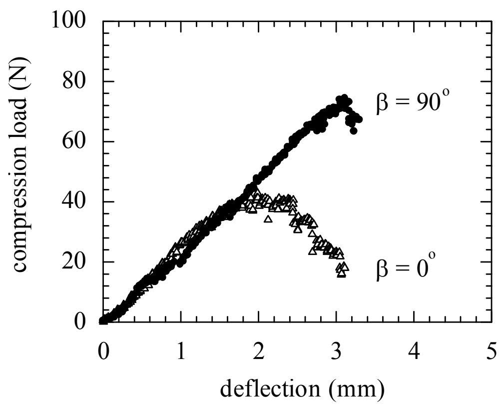

Fig. 3 Load-deflection relationship of fracture toughness tests

3.2 Fracture toughness, K_{IQ} and K_{IIQ}

The relationships between the mode I and mode II fracture toughness (K_{IQ} and K_{IIQ}) and mode-mixity angles (β) are shown in Fig. 4. To eliminate the effect of the variation of foam density, the fracture toughness were normalized by the relative density (ρ^*), i.e. the ratio between actual density (ρ_a) and expected density (ρ_e = 130 kg/m^3) of each specimen.

From Fig. 4(a), K_{IQ} was highest at β = 0° (pure mode I loading) then decreased continuously with increasing mode-mixity angle. At β = 90° (pure mode II loading), K_{IQ} became zero. On the other hand, K_{IIQ} was zero at pure mode I loading and increased gradually until β = 45°. For β > 45°, the steady state of K_{IIQ} was observed, i.e. K_{IIQ} was hardly sensitive to the mode-mixity angle (Fig. 4(b)).

The relationship between the normalized K_{IQ} and K_{IIQ} is shown in Fig. 5. The 45° dashed line is used to divide the mode of fracture into 2 regimes, e.g. the regime of dominated mode I loading above the dashed line and the regime of dominated mode II loading beneath the dash line. For the regime of dominated mode I, K_{IQ} decreased gradually as the combination of K_{IIQ} increased. Then, a sudden drop of K_{IQ} was observed at β = 45° (the transition from the regime of dominated mode I loading to the regime of dominated mode II loading). However, in the regime of dominated mode II loading, K_{IIQ} was insensitive to the drop of K_{IQ}.

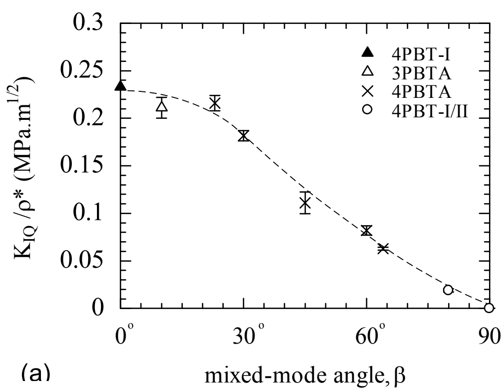

(a)

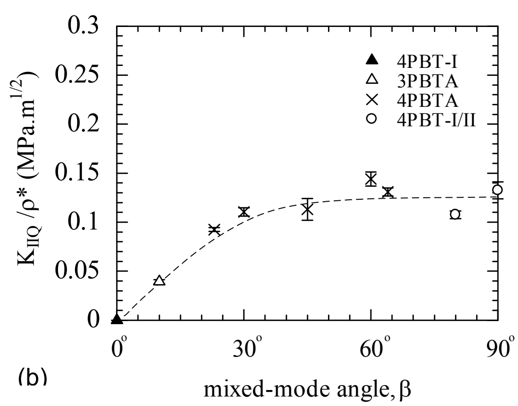

(b)

Fig. 4 (a) Relationship between normalized mode I stress intensity factors (K_{IQ}/ρ^*) and mode-mixity angle, (b) Relationship between normalized mode II stress intensity factors (K_{IIQ}/ρ^*) and mode-mixity angle

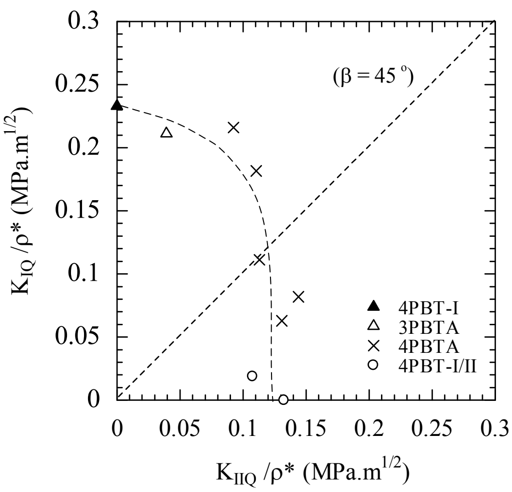

Fig. 5 Relationship between normalized stress intensity factors K_{IQ}/ρ^* and K_{IIQ}/ρ^*

In order to validate the applicability of the linear elastic fracture mechanics (LEFM) or using of K, the plastic zone (r_p) should not exceed the geometrical limitation in the ligament area of the specimen, which means

$$r_p < a, (W-a), b \tag{21}$$

The plastic zone (r_p) can be estimated using Irwin's plastic zone model, as following [9].

$$r_p = \frac{1}{\pi}\left(\frac{K_{IQ}}{\sigma_y}\right)^2 \tag{22}$$

where σ_y is the yield strength of the foam (1.292 MPa) [10]. From the calculation, only the plastic zone size under pure mode I loading (10.36 mm) was larger than the ligament area; i.e. the LEFM and the fracture toughness value (K_{IQ}) was not applicable. For the case of inelastic crack tip condition, the elastic-plastic fracture mechanics must be applied.

Under the dominated mode I loading (β < 45°), the Poisson contraction in the thickness direction could occur around the crack tip due to the lack of constraint on through-thickness deformation. The state of strain around the crack tip was three-dimensional, while the state of stress around the crack tip was two-dimensional (plane stress). Significant plastic deformation in the vicinity of crack tip resulted in the increasing of crack tip radius (crack blunting). Crack blunting reduced the severity of the crack and led to the increasing of fracture resistance [11].

From the observations during the tests (Fig. 6), crack tip blunting before the fracture of specimen was observed under pure mode I loading (β = 0°). On the other hand, under pure mode II loading, the crack tip did not open; and the sharp crack tip was observed, which led to the low fracture resistance (Fig. 5).

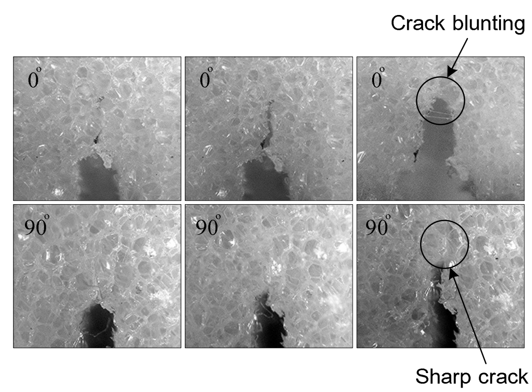

Fig. 6 (upper) Crack tip deformation under pure mode I fracture toughness test (β = 0°) and (lower) Crack tip deformation under pure mode II fracture toughness test (β = 90°)

3.3 Observation of fracture surfaces

After the fracture toughness tests, fracture surfaces were observed using an SEM. A substantial Poisson contraction was likely to occur for the dominated mode I loading. The Poisson contraction could lead to the compression and buckling of cell walls in the thickness direction. Evidences of compression and buckling of cell walls are shown in Fig. 7. The observation has been made in the areas near the notch tip, as schematically shown in Fig. 8(a). The buckling-cell ratio was defined as a ratio between the average number of buckling cells and the average number of overall cells. The relationship between the buckling-cell ratio and mode-mixity angle is shown in Fig. 8(b). The number of buckling cells decreased with increasing the mode-mixity angle. The results indicated that the Poisson contraction in the thickness direction (cell-wall buckling) could easily occur under the dominated mode I loading. Consequently, it led to the reduction of the severity of the crack due to the state of plane stress around the crack tip, i.e. high fracture toughness (Fig. 5).

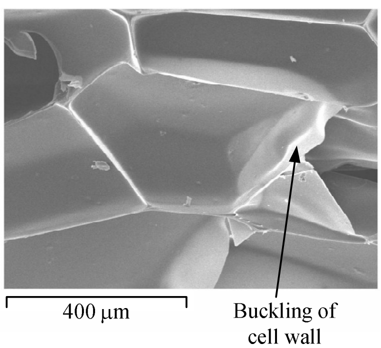

Fig. 7 Buckling cell observed from fracture surface of specimen tested under β = 30°

The SEM micrographs on the cell edges of the fracture surfaces of specimens tested at β = 0° and 90° were shown in Fig. 9. The different fracture surfaces were observed. For pure mode I loading, a rough fracture surface on the cell edge (Fig. 9(a)) was observed due to stretching on the cell edge from the crack tip opening. The evidence of stretching on cell edge could enhance the mechanism of crack blunting and led to higher fracture resistance for pure mode I loading (Fig. 5). On the other hand, for pure mode II loading, the crack tip did not open (Fig. 6), thus the deformation was likely to occur under shear loading with a relatively flat fracture surface as shown in Fig. 9(b). So, under the pure mode II loading, the crack tip condition was severe due to the sharp crack which resulted in the low fracture toughness (Fig.5).

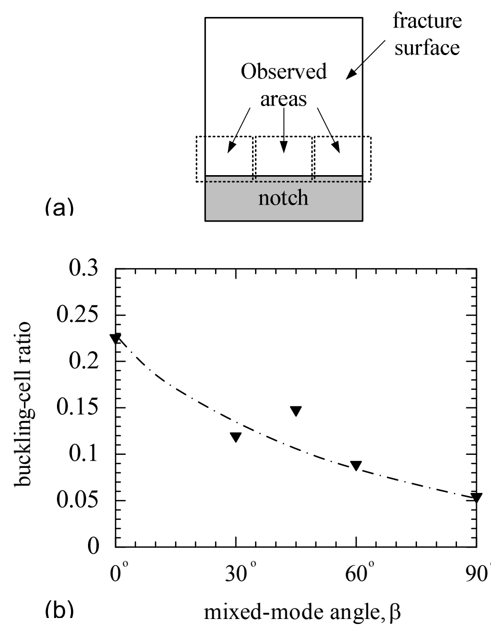

Fig. 8 (a) The observation areas for buckling cells and (b) plot of buckling-cell ratio

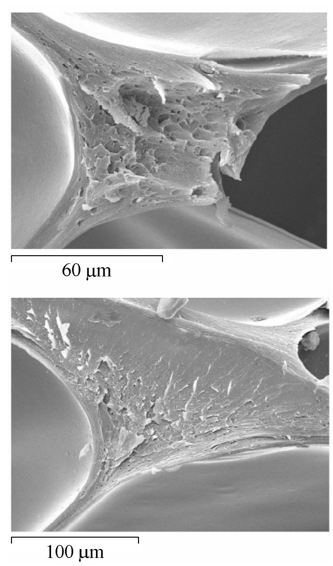

Fig. 9 Micrographs of fracture surfaces of specimens tested under (a) pure mode I loading (β = 0°) and (b) pure mode I loading (β = 90°)

4. Conclusion

In this work, the fracture behaviors of the closed-cell PVC foam (DIAB H130) under mixed-mode I/II loading have been studied. The findings can be summarized as follows.

1. Under pure mode I loading, the evidence of plastic deformation was observed before the fracture occurred. However, under pure mode II loading, linear relationship between load and deflection with the insignificant deformation was observed. The observation of crack tip deformation and the micrographs of fracture surfaces indicated that, under the opening mode, the crack tip was stretched and led to the crack blunting.
2. It was found that K_{IQ} decreased with increasing mode-mixity angle. While, K_{IIQ} increased with increasing mode-mixity angle from 0° to 45°, and became insensitive to the change of the mode-mixity angle above 45°.
3. The fracture toughness under pure mode I loading (K_{IQ}) was about 2 times larger than that under pure mode II loading (K_{IIQ}). From the observation of fracture surfaces, under pure mode I loading, cell wall buckling occurred widely which led to the reduction of the severity of the crack due to the state of plane stress around the crack tip. Otherwise, the buckling of cell walls hardly occurred under pure mode II loading; and the state of stress at the crack tip was plane-strain which led to the reduction of fracture resistance.

5. Acknowledgement

The authors would like to acknowledge the discussions and supports from the Office of the Higher Education Commission (Thailand), the Thailand Research Fund (TRF), the National Research Council of Thailand (NRCT), and the National Metal and Materials Technology Center (MTEC).

6. References

[1] Viana, G.M. and Carlsson, L.A. (2002). Mechanical properties and fracture characterization of cross-Linked PVC foams, *Journal of Sandwich Structures and Materials*, Vol. 4, pp. 99-113.

[2] Kabir, M.E., Saha, M.C., and Jeelani, S. (2006). Tensile and fracture behavior of polymer foams, *Materials Science and Engineering A*, Vol. 429, pp. 225-235.

[3] Noury, P.M., Shenoi, R.A., and Sinclair, I. (1998). On mixed-mode fracture of PVC foam, *International Journal of Fracture*, Vol. 92, pp. 131-151.

[4] ASTM (1993). Annual Book of ASTM Standards: D5045 – 93 Standard Test Methods for Plane-Strain Fracture Toughness and Strain Energy Release Rate of Plastic Materials.

[5] Murakami, I. (1987). Stress Intensity Factors Handbook, Pergamon Press, New York.

[6] Fett, T. (1991). Mixed-mode stress intensity factors for three-point bending bars, *International Journal of Fracture*, Vol. 48, pp. R67-R74.

[7] Choi, S.R., Zhu, D., and Miller, R.A. (2005). Fracture behavior under mixed-mode loading of ceramic plasma-sprayed thermal barrier coatings at ambient and elevated temperatures, *Engineering Fracture Mechanics*, Vol. 72, pp. 2144-2158

[8] He, M.Y. and Hutchinson, J.W. (2000). Asymmetric four-point crack specimen, *Journal of Applied Mechanics*, Vol. 67, pp. 207-209.

[9] Anderson, T.L. (1995). Fracture Mechanics Fundamental and Applications, CRC Press, Florida.

[10] Poapongsakorn, P. and Kanchanomai, C. (2010). Time-dependent deformation of closed-cell PVC foam, *Journal of Cellular Plastics*, in press.

[11] Kanchanomai, C. and Rattananon, S. (2008). Effects of loading rate and thickness on mixed-mode fracture toughness of thermoset epoxy resin, *Journal of Applied Polymer Science*, Vol. 109, pp. 2408-2416.